Electronic Supplementary Information (ESI)

Lab Chip, (2017), DOI: 10.1039/c6lc01516f.

Coplanar electrode microfluidic chip enabling high-accuracy sheathless impedance cytometry†

Adele De Ninno,‡[a] Vito Errico,‡[a] Francesca Romana Bertani,[b] Luca Businaro,[b]

Paolo Bisegna,*[a] and Federica Caselli*[a]

[a] *Department of Civil Engineering and Computer Science, University of Rome Tor Vergata*

E-mail: caselli@ing.uniroma2.it, bisegna@uniroma2.it

[b] *Institute for Photonics and Nanotechnologies, Italian National Research Council*

‡These authors contributed equally to this work.

*Corresponding authors.

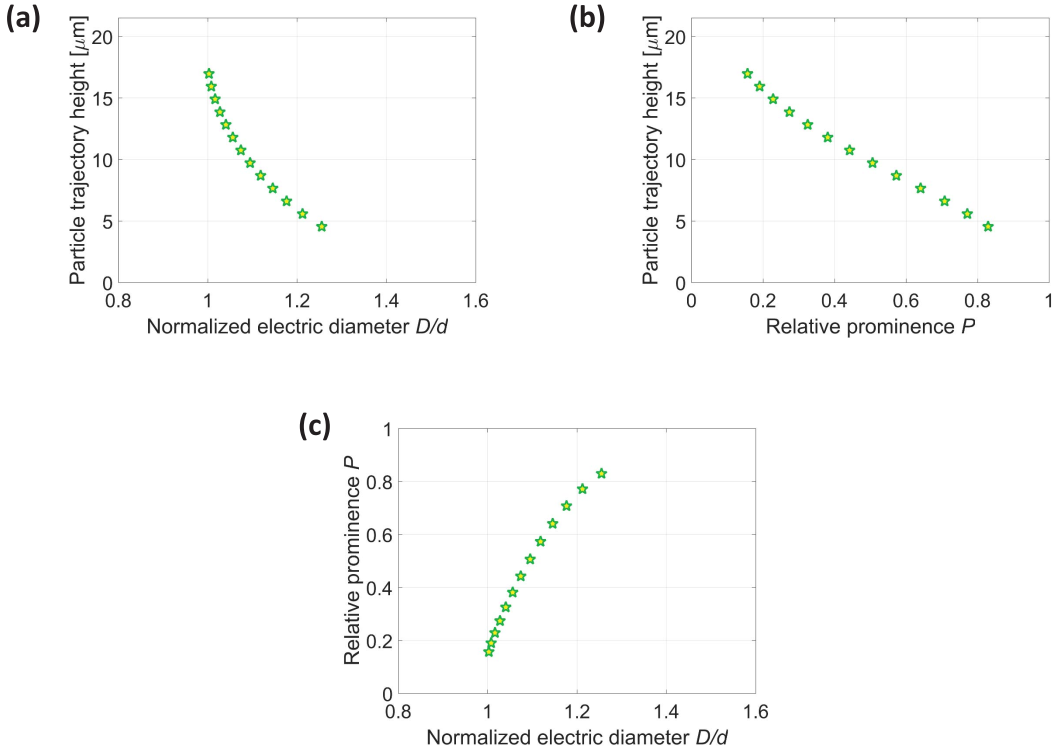

Figure S1: Simulation results (6 μm diameter beads). (a) Particle trajectory height vs electrical diameter D normalized by nominal bead diameter d. A significant spread in D/d is found, with trajectories close to electrodes providing higher values than trajectories far from electrodes. (b) Particle trajectory height vs relative prominence P. An almost linear regression is found, suggesting that P can be a suitable metric to estimate the particle trajectory height. (c) Relative prominence P vs normalized electrical diameter D/d (cf Figure 5 of main text).

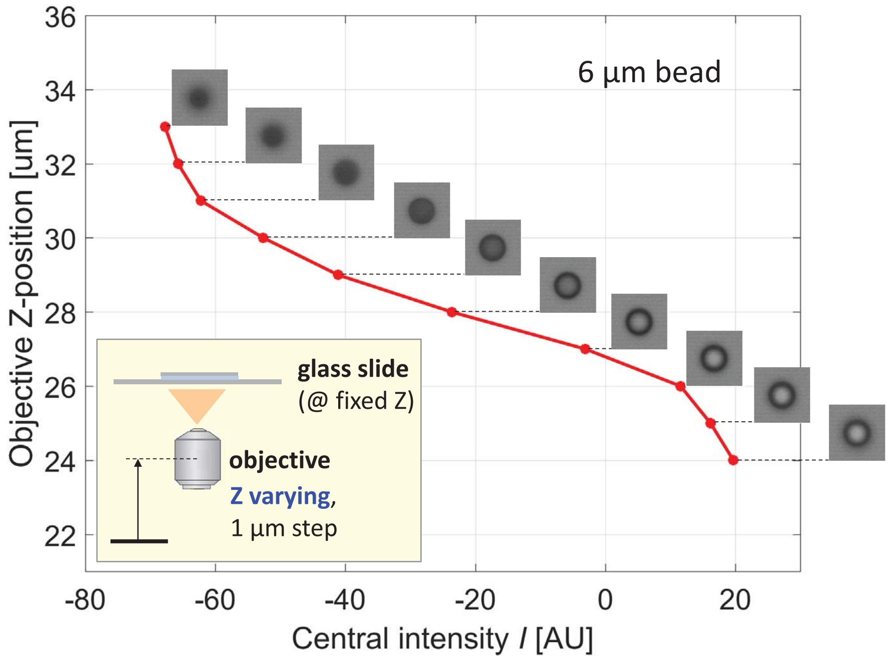

Figure S2: Calibration curve of bead defocusing. A drop of 6 μm diameter polystyrene beads suspended in PBS was pipetted onto a glass slide, covered with a cover slip and placed on the stage of an inverted microscope (held at a fixed Z-position). Bright-field microscopy images of one bead (55$\times$55 pixels) were acquired at different Z-position of the imaging system focal plane (1 μm step Z-displacement of the microscope objective). The central intensity I of the bead image (average intensity computed over a centered 6 pixel diameter circle) is reported against the Z-position of the microscope objective. The bead respectively produces an image with low / intermediate / high central intensity when it is below / on / above the focal plane (i.e., high / intermediate / low objective Z-position). Materials: Zeiss Axio Observer Z1 microscope (40$\times$ objective), Photron Mini UX100 camera.

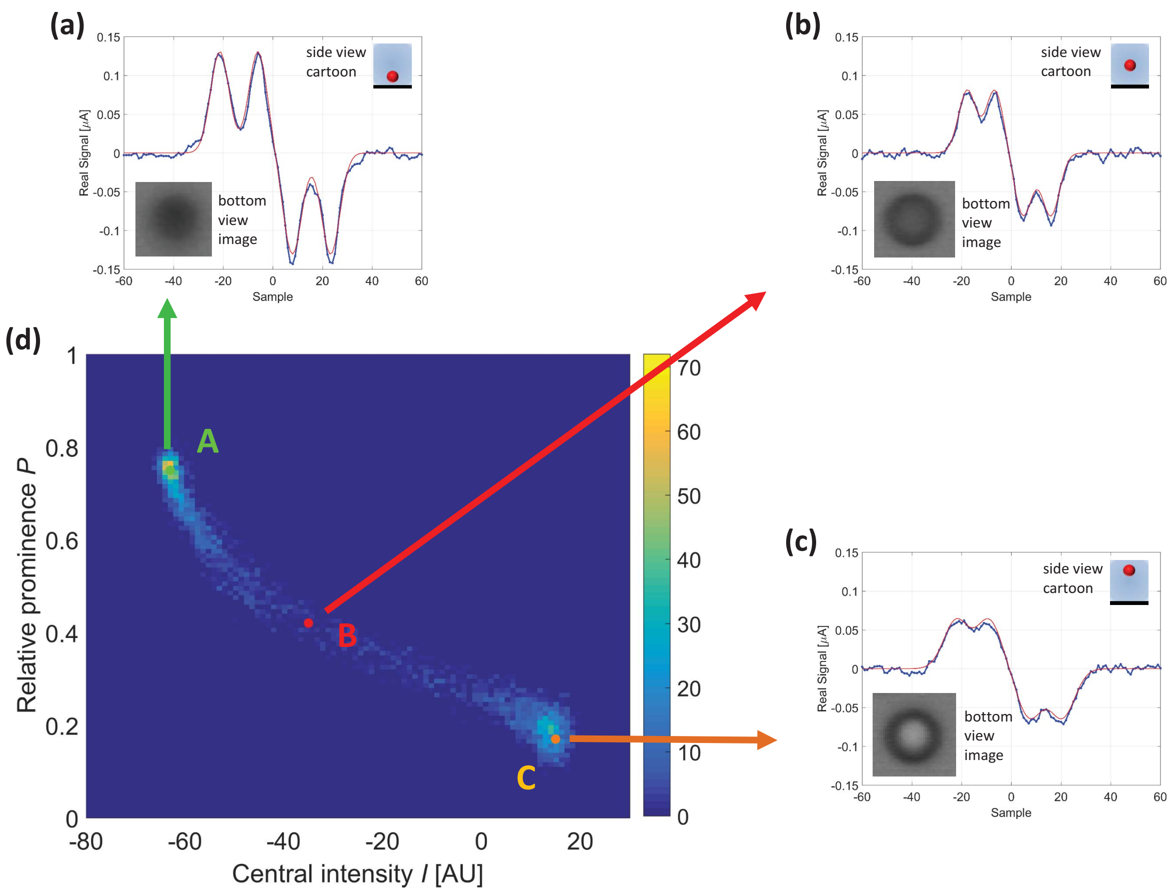

Figure S3: A suspension of 6 μm diameter beads in PBS was pumped through the device (concentration 10^3 beads per μl, flow rate 10 μl/min). Impedance signal was recorded as described in Section 3 of the main text. Bottom view images of the flowing beads were acquired using a Photron Mini UX100 camera (frame rate 2000 fps, shutter time 3.9 μs) connected to a Zeiss Axio Observer Z1 inverted microscope (40$\times$ objective). The objective focal plane was adjusted to the middle of the channel. Events detected in the impedance datastream were matched to their optical images with a custom Matlab script. The exemplary events in panels (a), (b), (c), respectively exhibit high / intermediate / low prominence. Because their images have low / intermediate / high central intensity, their trajectory heights turn out to be below / on / above the focal plane (Figure S2), i.e., close to the electrodes / through the middle of the channel / close to the top of the channel. (d) Density plot of the beads, with the relative prominence P of the impedance signal plotted against the central intensity I of the matched optical images. Because I encodes for particle trajectory height (Figure S2), the observed relationship between P and I proves that the relative prominence P is a new impedance-based metric encoding for particle trajectory height.

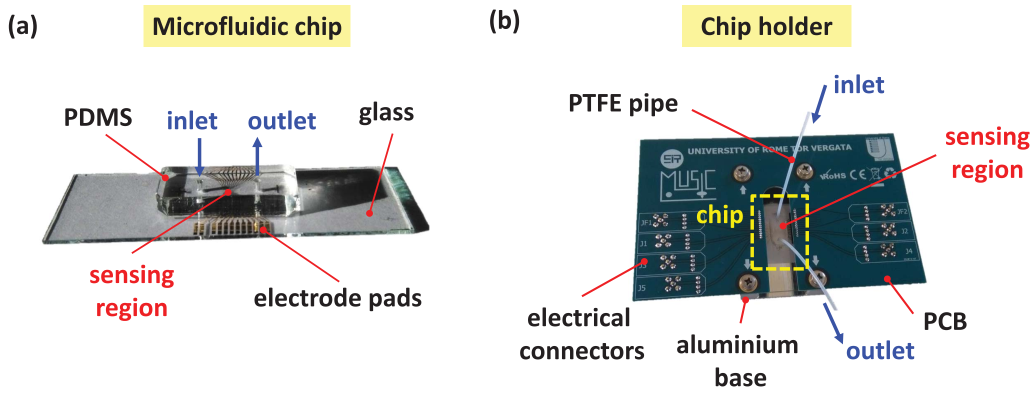

Figure S4: (a) Photograph of the microfluidic impedance chip, consisting of a PDMS (polydimethylsiloxane) fluidic top layer and patterned microelectrodes in a coplanar configuration on glass (additional electrodes are present, that were not used in the present work). (b) Chip holder for electrical and fluidic connections.

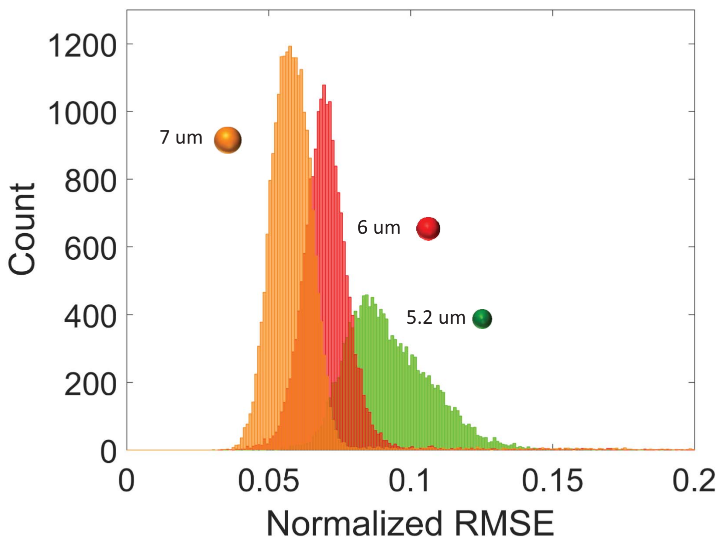

Figure S5: Fitting accuracy of the bipolar double-Gaussian template (equation (1) of the main text) to the experimental traces (suspensions of 5.2, 6 and 7 μm diameter beads measured separately). The histogram of the root mean squared error of the fit (RMSE), normalized by peak amplitude control a is plotted, showing good fitting accuracy of the template.

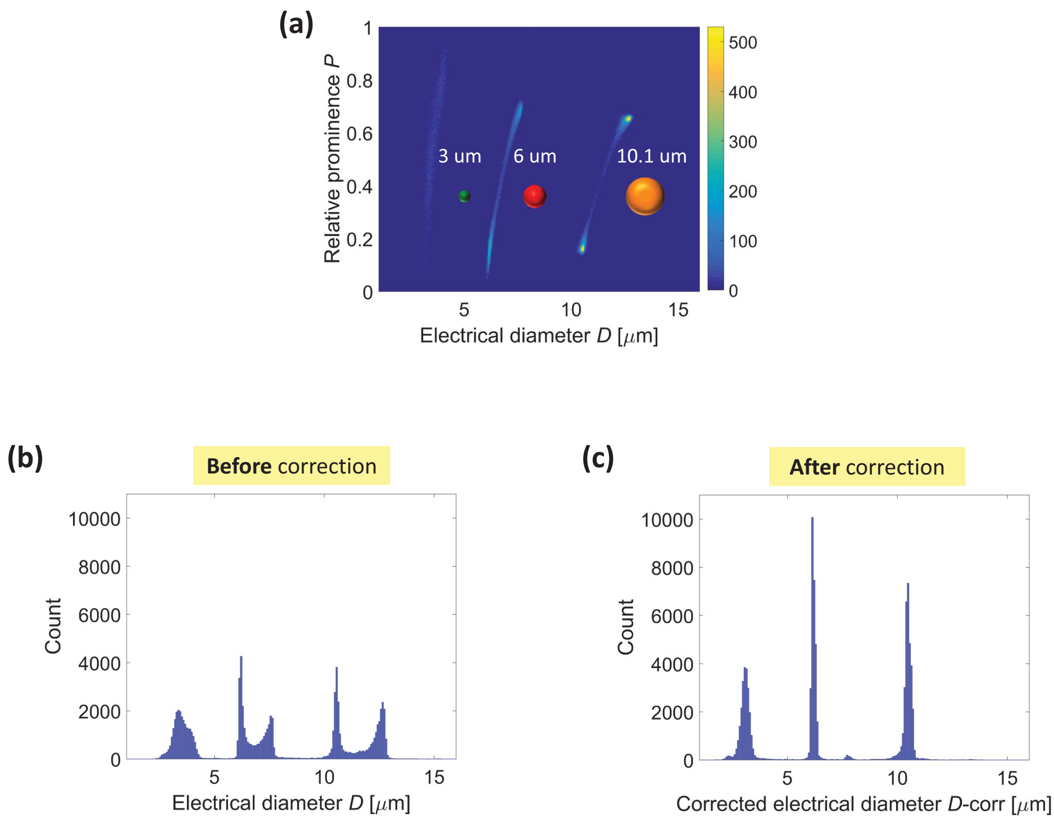

Figure S6: (a) Density plot of a mixture of 3, 6 and 10.1 μm diameter beads, with the relative prominence P plotted against the electrical diameter D. Histogram of the electrical diameter (b) before and (c) after compensation (parameters reported in Table 1 of the main text, last row). Results in panel (c) show that the proposed compensation procedure is effective also for 3 and 10.1 μm diameter beads, and that the detection limit of the device is below 3 μm.

1 The relative prominence

The expression of the relative prominence P reported in equation (7) of the main text is here derived.

By substituting equation (6) of the main text into equation (5) of the main text, it follows that

$$P = 1 - \frac{2s(t_c - \delta/2)}{s(t_c - \delta/2 - \gamma/2) + s(t_c - \delta/2 + \gamma/2)} \,. \tag{1}$$

Then, using equation (1) of the main text, it turns out that

$$P = 1 - \frac{2(g(0) - g(-\delta))}{g(-\gamma/2) - g(-\delta - \gamma/2) + g(\gamma/2) - g(-\delta + \gamma/2)} \,. \tag{2}$$

Using equation (2) of the main text, and recalling that $\sigma \ll \delta$, it turns out that $g(-\delta)$, $g(-\delta - \gamma/2)$, and $g(-\delta+\gamma/2)$ can be respectively neglected with respect to $g(0)$, $g(-\gamma/2)$, and $g(\gamma/2)$. Accordingly, P is transformed into:

$$P = 1 - \frac{2g(0)}{g(-\gamma/2) + g(\gamma/2)} \,, \tag{3}$$

which can be recast into

$$P = 1 - \frac{2e^{-\gamma^2/(8\sigma^2)}}{1 + e^{-\gamma^2/(2\sigma^2)}} \tag{4}$$

Except at most for low values of the relative prominence, the quantity $e^{-\gamma^2/(2\sigma^2)}$ is negligible with respect to 1, so that the following expression is derived:

$$P = 1 - 2\,e^{-\gamma^2/(8\sigma^2)} \,, \tag{5}$$

reported in equation (7) of the main text.

It is pointed out that both equations (4) and (5) yield effective metrics that can be used to compensate for the spread in signal amplitude characterizing nominally identical particles flowing at different heights. In fact, those metrics are function of the ratio γ/σ, which in turn can be used as an effective metric too, up to a straightforward modification of the calibration procedure. In this work, the expression (5) has been preferred, as it shares both simplicity and clear geometrical interpretation.